RSC Advances

REVIEW

View Article Online
View Journal | View Issue

Cite this: *RSC Adv.*, 2023, **13**, 16512

Hydroxyapatite-based carriers for tumor targeting therapy

Gongming Qian, *[ab] Lingya Xiong [a] and Qing Ye*[ab]

At present, targeted drug delivery is regarded as the most effective means of tumor treatment, overcoming the lack of conventional chemotherapeutics that are difficult to reach or enter into cancer cells. Hydroxyapatite (HAP) is the main component of biological hard tissue, which can be regarded as a suitable drug carrier due to its biocompatibility, nontoxicity, biodegradation, and absorbability. This review focuses on the cutting edge of HAP as a drug carrier in targeted drug delivery systems. HAP-based carriers can be obtained by doping, modification, and combination, which benefit to improve the loading efficiency of drugs and the response sensitivity of the microenvironment in the synthesis process. The drug adsorbed or *in situ* loaded on HAP-based carriers can achieve targeted drug delivery and precise treatment through the guidance of the *in vivo* microenvironment and the stimulation of the *in vitro* response. In addition, HAP-based drug carriers can improve the cellular uptake rate of drugs to achieve a higher treatment effect. These advantages revealed the promising potential of HAP-based carriers from the perspective of targeted drug delivery for tumor treatment.

Received 6th March 2023
Accepted 18th May 2023

DOI: 10.1039/d3ra01476b

rsc.li/rsc-advances

1. Introduction

Malignant tumors are one of the major diseases that seriously affect human health and threaten human life.[1] At present, the treatment of malignant tumors mainly includes surgery, radiotherapy, chemotherapy, targeted therapy, and immunotherapy. Among them, local treatment, such as surgery and radiotherapy, can only work for the primary and some metastatic sites of malignant tumors, but it cannot completely cure the tumors transfer to other parts through the blood or lymphatic system. Chemotherapy belongs to systemic treatment, which can treat all tumor cells. However, the selectivity of chemotherapy drugs usually is poor, which cannot clearly distinguish between normal cells and tumor cells, resulting in damage to normal tissues during treatment.[2] Targeted therapy and immunotherapy represent the biggest breakthrough and progress in tumor treatments. Immunotherapy is becoming a powerful tumor treatment method by activating the human immune system and relying on its own immune function to kill tumor cells. However, there are still many challenges in the widespread implementation of immunotherapy, such as its serious adverse reactions and non-specific and autoimmune inflammation.[3] Targeted therapy refers to the formation of high concentrations of targeted drugs at tumor sites through selective binding with carcinogenic sites. In this way, the effects of drugs on tumor cells can be improved and the toxicity to surrounding normal cells can be reduced.

According to different targeting mechanisms, drug targeting can be divided into passive targeting, active targeting, and physical targeting. Passive targeting is achieved by enhancing cellular tissue permeability and the retention effect of the drug by regulating the composition, particle size, charge, and other characteristics of the carrier. Active targeting is making tumor marker molecules loaded onto the carrier to improve the ability to identify and combine with tumor cells. Physical targeting is regulating the distribution and release characteristics of drugs in the body depending on the responsiveness of the drug carrier to the physical signals, such as light, heat, magnetic, electric, and ultrasonic waves.[4] Therefore, one key technology for targeting drugs is the design of drug carriers. The common drug carriers used for targeting drug delivery include natural polymers, liposomes, micelles, and inorganic materials, as shown in Table 1. Among them, inorganic nanomaterials have received widespread attention due to the advantages of easy morphology regulation, multifunctional properties, performance stability, and simple preparation processes.

Hydroxyapatite (HAP, $Ca_{10}(PO_4)_6(OH)_2$) is a kind of phosphate that is the main component of hard tissue of vertebrates with a hexagonal columnar structure. The special crystal structure maintains two types of crystal planes with different charges. The high surface activity is beneficial for drug adsorption and loading.[11] In addition, HAP has excellent biocompatibility and bioactivity, which can be widely applied in the field of biomedicine,[12,13] hard tissue repairing and replacing materials.[14,15] In recent years, HAP nanoparticles (HAP NPs) as

[a]*College of Resource and Environmental Engineering, Wuhan University of Science & Technology, Wuhan 430081, China. E-mail: qiangongming@wust.edu.cn*
[b]*Hubei Key Laboratory for Efficient Utilization and Agglomeration of Metallurgic Mineral Resources, Wuhan University of Science and Technology, Wuhan 430081, China. E-mail: yeqing@wust.edu.cn*

Table 1 Characteristics of different carriers used for drug delivery

Drug carrier	Representative materials	Advantage	Disadvantage	Ref
Natural polymers	Polysaccharides (*e.g.*, chitosan, carrageenan, alginates, *etc.*)Proteins (*e.g.*, collagen, gelatin, and silk fibroin, *etc.*)	Economical, readily available, non-toxic, and potentially biodegradable	The separation and purification processes are complex	5 and 6
Liposomes	Phosphatidylcholine, phosphatidic acid, octadecanamide, cholesterol, *etc.*	Increasing the stability of the drug and reducing its toxicity	Easily cleared from the bloodstream by the lymphatic and reticuloendothelial systems	7
Micelles	Polyethyleneglycol (PEG), polyamide (PA), polyoxyethylene (PEO), *etc.*	Large drug loading space, increasing the solubility of insoluble drugs and facilitating body metabolism	Poor transport performance for solubility drugs	8
Dendrimers	Polyamidoamine, poly(L-lysine), polyethylenimine, poly(propylene imine), *etc.*	Active functional groups enriched on the surface and have spacious internal cavity structures	Non-degradability and accumulation in the body	9
Inorganic nanoparticles	Fe_3O_4, Au, carbon nanotube, hydroxyapatite, *etc.*	Multifunctional, high specific surface area, large pore volume	Poor biodegradability	10

a drug carrier, have attracted more and more attention. Compared with other drug carriers, HAP is easier to load and release drugs *in vivo* delivery.[16–19] Also, HAP could decompose to release Ca^{2+}, inducing the apoptosis of tumor cells and improving tumor treatment efficiency.[20] As such, HAP is a promising drug carrier.

This review provides an overview of the common synthesis, modification, doping, and recombination methods of HAP for tumor targeting therapy. The detailed preparation process and application of targeted HAP-based carriers with pH response, thermal response, magnetic response, and light response are shown in Fig. 1. Due to the excellent biocompatibility and bioactivity of HAP, the potential synergistic effects of HAP-based drug carriers in tumor treatment and the potential side effects on the body have been discussed.

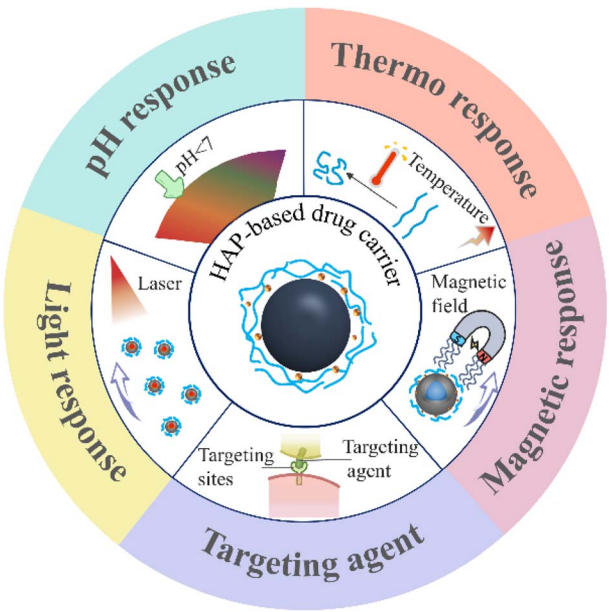

Fig. 1 Schematic diagram of the responsiveness of HAP-based carriers.

2. Preparation of HAP-based carriers

There are many ways to prepare HAP, but using it as a drug carrier, shape, drug loading capacity, biocompatibility, and other special responsiveness must be considered.

2.1 Synthesis of HAP nanoparticles

As an ideal medical material, the preparation of HAP NPs with high purity, good dispersion, stable performance, and controllable size and morphology has become an important research project. The raw materials used to synthesize HAP can be classified as natural source materials and chemical materials. Natural materials include mammalian bones, fish scales, bones, shells, and mineral resources.[21] As for chemical materials, calcium salts and phosphate salts including $Ca(NO_3)_2 \cdot 4H_2O$, CaO, $CaCl_2$, and $(NH_4)_2HPO_4$, H_3PO_4, NaH_2PO_4 have been used as raw materials for HAP synthesis. Different preparation methods require a variety of raw materials to obtain HAP NPs with diverse properties. In comparison, the synthesized HAP could realize crystal morphology regulation using chemical agents. At present, the main preparation methods of HAP NPs can be divided into the dry method and the wet method.[22–24] The solid-state method is a kind of the typical dry method, which involves calcining precursors containing calcium and phosphate-based on the ion solid diffusion.[25] However, HAP NPs prepared by the solid-state method show poor activity and often contain impurities.[26] In comparison, HAP NPs prepared using wet synthesis including the sol–gel method, chemical precipitation, hydrothermal synthesis, and

Table 2 Main preparation methods of HAP

	Synthetic method	Advantage	Disadvantage
Dry synthesis	Solid-state method	Fully dispersed, low-cost, and a simple preparation process	High energy consumption, large particle size, and poor activity of generated powder
	Mechanochemical method	Obtain specific-sized powders	Lower purity
Wet synthesis	Sol–gel method	Simple and economical, good uniformity, and better biocompatibility	Complex process flow, lower production efficiency
	Coprecipitation method	Simple operation, easy to introduce ions, low crystallinity, and good activity	Easy to generate other impurities, irregular product morphology, and poor dispersibility
	Hydrothermal method	High crystallinity and purity, low cost, and easy to operate	The morphology and particle size of crystals are difficult to control, strictly reaction conditions
	Template method	Effectively design and regulate the morphology, and enhance the drug loading capacity	The structure is prone to damage

template method can effectively control the morphology and the particle size, which is beneficial to achieve better drug loading and sustained release. A brief summary of various preparation methods is shown in Table 2.

In wet synthesis, the sol–gel method uses highly chemically active components as precursors and generates a stable transparent sol system through hydrolysis. After aging, the sol slowly polymerizes to form a gel, then the nanostructured materials can be prepared using the drying-sintering-solidification process (Fig. 2(a)).[27] The phase composition, crystallinity, and grain size of HAP NPs increased with the increase in the calcination temperature.[28] The sol–gel method is simple and economical, and the production has good homogeneity and better biocompatibility. However, the process is complex with low productivity. The coprecipitation method is based on the precipitation reaction between calcium salts and phosphates salts. For example, $Ca(OH)_2$ is commonly used as a raw material to prepare the suspension. After vigorous stirring, H_3PO_4 solution is slowly added to form precipitation and adjust pH using ammonia solution. Then, HAP particles were obtained after filtration and drying.[29] The synthesized HAP particles gather and grow along the *c*-plane using the coprecipitation method with low crystallinity and high activity. The long axis of the obtained HAP with the increased Ca/P ratio in the initial solution.[30,31] Hydrothermal synthesis is another method of synthesizing HAP in an aqueous solution or steam at high temperature and high pressure. HAP nanorods with uniform size can be synthesized by adding alanine and glutamic acid, and the particle size of HAP can be controlled.[32] Compared with glutamate, HAP particles were fully dispersed with higher crystallinity in the presence of alanine. The HAP product of hydrothermal synthesis also has high purity, which can be used as drug carriers with specific particle sizes. Moreover, the hydrothermal method is an effective method for preparing sheet-shaped HAP with *a*-plane orientation by adjusting the Ca/P ratio and pH value, which is beneficial for the loading of specific drugs.[33,34]

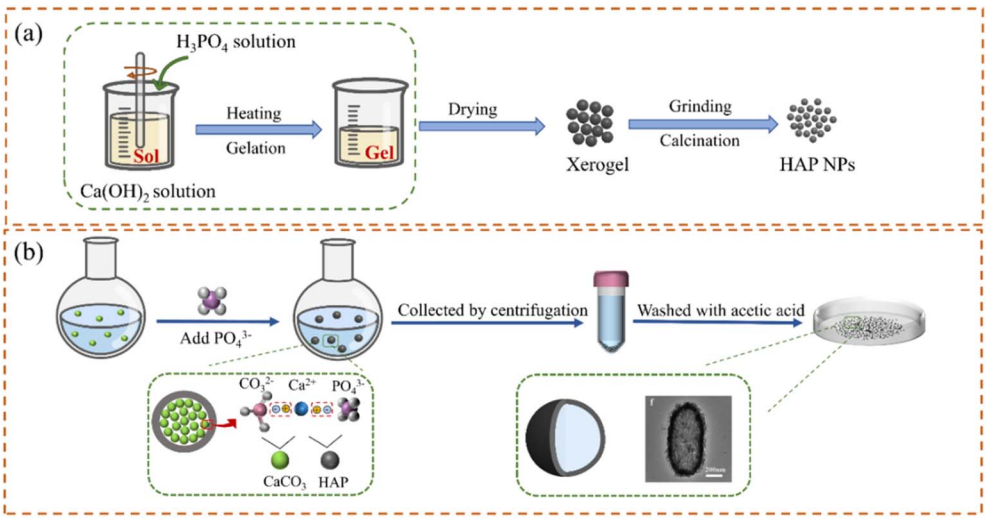

Fig. 2 Preparation of HAP NPs by (a) sol–gel method and (b) template ($CaCO_3$) method.

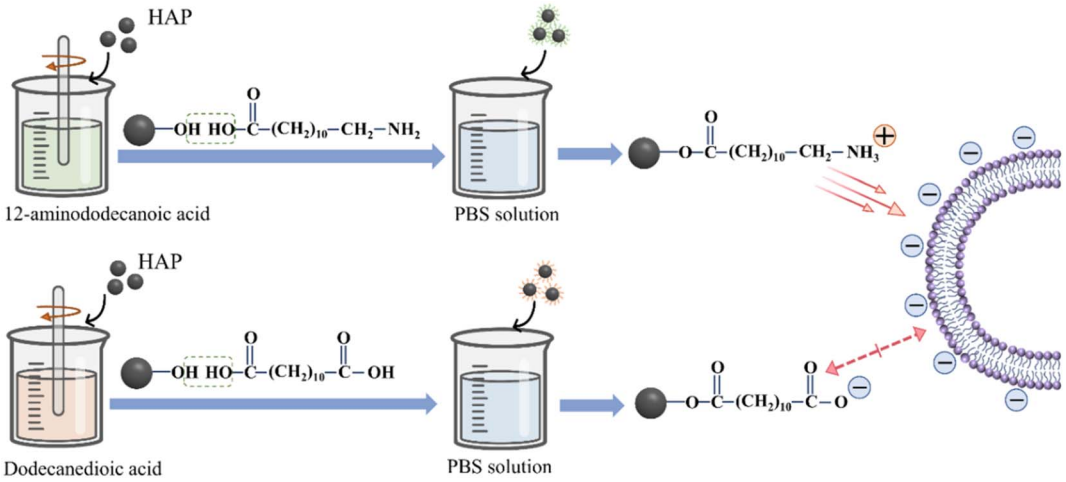

Fig. 3 Modification of the surface charge of HAP NPs.

To reduce the agglomeration and control the size of HAP particles, special organic or inorganic materials are usually added as templates to prepare HAP NPs with high specific surface area and (or) to develop porous structures for improving the drug loading capacity.[35,36] For example, polyacrylic acid (PAA) with a large number of carboxyl groups can provide complexing sites for the nucleation of Ca^{2+} and afford steric hindrance. When used as a template, the tiny calcium phosphate nuclei were first generated along the polycarboxylate chain and then self-assembled into spherical nanoclusters on the polymer template. It can elevate the stability and dispersibility of HAP NPs in the synthesis process. Therefore, HAP NPs with spherical structure and low crystallinity could be obtained.[37] Using block copolymer F127 as a template, rod HAP with a mesoporous structure of 75–125 nm in length and about 25 nm in diameter can be synthesized by adjusting the dosage of polymer, precursor concentration, and reaction time.[38] Compared with spherical HAP NPs, rod HAP NPs have longer blood circulation time.[39] Alternately, HAP NPs with hollow structures can be synthesized using inorganic templates, which are widely used in drug carriers.[40,41] At first, calcium and phosphorus ions are precipitated on the pre-synthesized nanocarbon template and then after eliminating the template's core carbon structure through calcination, nanostructured hollow HAP NPs were formed.[42] Hollow HAP NPs have a high specific surface area, which benefits the drug delivery of different drugs and protein molecules. In addition, the HAP ellipsoid capsules with hollow and porous structures can be prepared with $CaCO_3$ as a template and calcium source (Fig. 2(b)).[43] After adding PO_4^{3+}, a HAP shell was formed on the surface of the $CaCO_3$ ellipsoid. Then, the remaining $CaCO_3$ core can be removed using dilute acetic acid. The size and shape of the HAP hollow capsule are determined by $CaCO_3$ core micromorphology. The thickness of the capsule shell depends on the added concentration of PO_4^{3+}. The synthesized HAP hollow ellipsoid capsule had a high specific surface area, high drug storage capacity, and good drug release efficiency.[44] The adjustment of crystal size and orientation of HAP can be realized through template synthesis, but it is necessary to consider the adverse effects of templates on health and therapy effects.

2.2 Modification of HAP-based carrier

Since the intracellular drug delivery of HAP NPs depends on cellular uptake, the interaction between HAP NPs and cells is very important for the design of HAP-based carriers in DDS. HAP NPs with different surface charges have different effects on cellular uptake, activity, and proliferation *in vitro*. As mentioned above, the amount of positive charges is higher than that of negative charges on the surface of rod HAP NPs, which has obvious advantages over spherical nanoparticles in terms of cellular uptake.[38,45] As such, the surface charge of HAP can be controlled by adjusting the crystal form and crystal size using different synthesis methods. Meanwhile, the surface charge of nanoparticles can be adjusted using surface modification such as 12-amino dodecanoic acid (positive) and dodecanedioic acid (negative) (Fig. 3).[46] In addition, reasonably designing the surface charges of HAP carriers is beneficial for the adsorption of various drugs. Adjusting the ions or pH in the buffer solution can directly control the adsorption of anions or cations on the surface of HAP.[47] For example, BSA and HAP generate electrostatic adsorption through the negative head on BSA and the positive calcium ion on HAP. When the environmental pH is low, the dissolution of HAP will disrupt the interaction, resulting in poor adsorption efficiency. As the pH increases from 7.5 to 9, the increasing negative charge on the surface of HAP hinders the adsorption of BSA.[48] Due to the presence of Ca^{2+} and PO_4^{3-} in HAP itself, positively and negatively charged drugs exhibit more favorable adsorption on Ca-deficient HAP and Ca-surplus HAP, respectively.[49]

The surface chemical modification of HAP can also introduce functional groups on the surface to facilitate the effective composition of the drug, targeting agent, and slow-release materials. For example, when polyethylene glycol (PEG) is coated on the HAP surface, the carboxylic acid group provided

by PEG enables folic acid (FA) to be transplanted to the distal end of PEG to target cancer cells. In addition, the HO-$(CH_2$-$CH_2O)_nH$ group can be introduced on the HAP surface to prevent the agglomeration of HAP NPs.[50] The special surface modification of HAP can also increase the effective combination with the anticancer drug cisplatin. The side carboxyl group of the multi-carboxyl HAP poly (AMA-COOH) outer layer can be coupled with the anticancer drug cisplatin to achieve drug loading. Through cytotoxicity tests, it was found that the HAP-poly (AMA-COOH) carrier without loading cisplatin exhibited little toxicity.[51] Similarly, $-NH_3^+$ on the surface of HAP modified with alendronate (AlN) can react with $-COO^-$ on IBU.[52] The HAP modified with AlN showed higher IBU storage capacity and relatively favorable drug release behavior. The chemical surface modification process maintained the raw structure of HAP and easily controlled the degree of functionalization. Therefore, the surface modification of HAP NPs can further optimize their biocompatibility and drug-carrying capacity and continuously enrich their advantages as drug carriers.

2.3 Doping of HAP-based carriers

The Ca^{2+}, PO_4^{3-} and OH^- ions of HAP can be easily replaced by ions and groups, which can improve its physical and chemical properties, such as conductivity, crystallinity, solubility, and thermal stability,[53,54] and even help to improve the drug loading and antibacterial ability of the HAP-based carrier (Fig. 4(a)). For example, compared with pure HAP NPs, the drug loading capacity of HAP NPs doped with Al^{3+} (Al-HAP) is significantly improved, and the loading capacity of doxorubicin (DOX) reached about 100 μg mg^{-1}.[55] The conducting biocompatibility experiments showed that the cell survival rate decreased from 98% to 88% as the concentration of Al-HAP increased from 0 to 1 mg mL^{-1}, which indicates that the addition of Al will have an impact on the biocompatibility of HAP. Due to the smaller ion radius of Mg^{2+} than that of Ca^{2+}, HAP NPs doped with Mg^{2+} (Mg-HAP) would generate lattice distortion and lattice size reduction, which can inhibit the nucleation and growth of HAP crystal. With the increase inMg^{2+} content, Mg-HAP had lower crystallinity, smaller grain size, larger solubility, and higher porosity.[56,57] When the substitute content of Mg^{2+} was 5.7%, Mg-HAP has better pysico-chemical features. The adsorption and release experiments of protein showed that after doping Sr^{2+} into HAP, the adsorption capacity for BSA and lysozyme (LYS) increased significantly compared to that of HAP.[58] Also, Sr-HAP has good sustained protein release ability. The protein release rate of Sr-HAP in the first 1 h was not more than 13.45%, which was significantly lower than that of HAP (about 20.98%). As such, it was conductive to be used as a drug carrier for sustained release administration.[59] The interactions of *in vitro* cell materials with osteoblast cells showed that Sr-HAP had significant bone compatibility and bone spur-stimulating growth without cytotoxicity.[60,61] Hence, HAP NPs doped with Sr^{2+} (Sr-HAP) are considered as an ideal protein drug carrier.

The antibacterial properties of drug carriers are conducive to the auxiliary drug inhibition of diseased cells. As such, developing antibacterial drug carriers is instrumental to improve the treatment effect. The HAP NPs doping with Ag^+ (Ag-HAP) showed good antibacterial activity against bacterial strains.[62,63] For example, Ag-HAP showed complete inhibition of *Escherichia coli* growth after 20 hours of culture and effective antibacterial activity against Gram-positive *Staphylococcus aureus* due to the anti-infective properties of heavy metals Ag. Experiments found that Ag-HAP nanoparticles did not show any toxic effect on MG-63 cells with loaded concentrations lower than 200 μg mL^{-1}. When the concentration was higher than 250 μg mL^{-1}, the cell viability decreased to 44%; that is, Ag-HAP exhibited strong

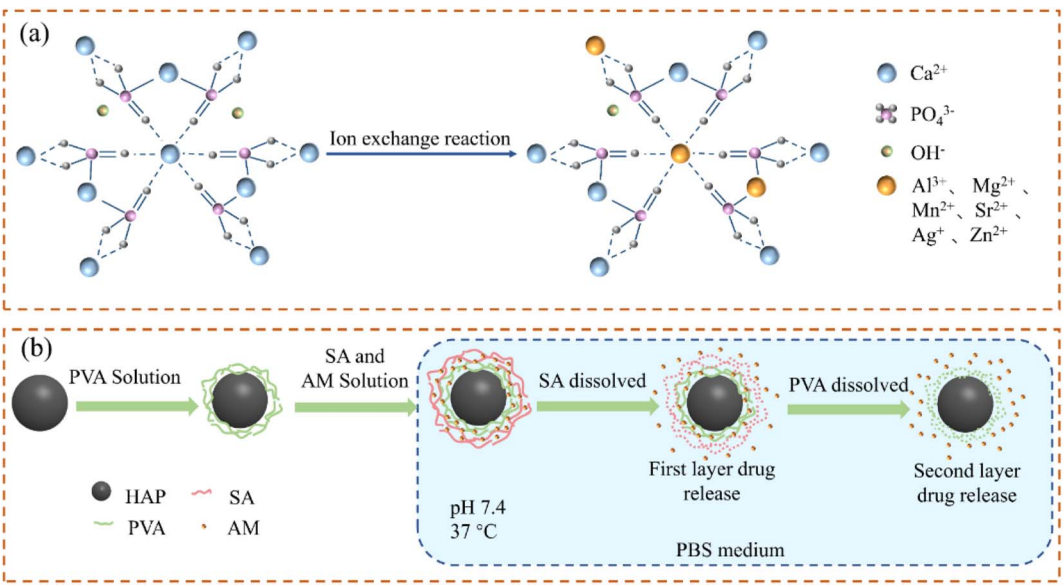

Fig. 4 (a) Schematic diagram of HAP structure of doped ions; (b) drug sustained-release process of the SA/PVA/HAP composite drug carrier.

Table 3 The summary of HAP-based doped carriers

Carrier	Preparation method	Morphology	Particle size (nm)	Ion ratio (mol%)	Cytotoxicity/antibacterial test	Optimized performance	Ref.
Al-HAP	Hydrothermal method	Rod-shaped	100–150	17.4	A549 cells	Increase the surface area and pore size	55
Mg-HAP	Coprecipitation method	—	~160	5.4–12.0	Osteoblasts	Osteoconductivity and resorption	63
Sr-HAP	Hydrothermal method	Rod-shaped	140–320	1–20	—	Increased protein loading and ability to release continuously	59
Ag-HAP	Double-emulsion method	Circular	~560	11.1–55.6	A549 cells, ATCC 25922, ATCC 6538	Showed good cytocompatibility and antibacterial activity	70
Zn-HAP	Ultrasonic synthesis	—	—	28.6	NIH-3T3 fibroblasts, ATCC 8799, ATCC 9027, ATCC 6538	Enhanced antibacterial effect and good cell adhesion and proliferation	65
F-HAP	Hydrothermal method	Nanorods	~50	33	MC3T3-E1, *E. coli*, Gram-negative, *S. aureus*, Gram-positive	Significantly increased crystallinity and demonstrated antibacterial properties	75
Si-HAP	Hydrothermal method	Rod-shaped	500	1	MC3T3-E1	Si-HAP has the effect of promoting cell proliferation and differentiation	69

antibacterial characteristics and showed cytotoxicity effects when loaded with highly concentrated amounts.[64] Clinical studies showed that Ag-HAP-coated implants for total hip arthroplasty with a maximum silver content of 2.9 mg per implant can prevent artificial joint infections. Another research showed that HAP-biphasic ZnO (Zn-HAP) can effectively inhibit the growth and development of bacteria and yeast fungi.[65] When Zn-HAP was 0.1 mg mL^{-1}, the survival rates of live cells of *E. coli* and *P. aeruginosa* were only 44% and 37%, respectively, while the mortality rates of two kinds of staphylococci were as high as 100%. The murine fibroblasts cultured with Zn-HAP showed good stability and seldom had cytotoxic effects on cellular structure and tissues. Therefore, Zn-HAP can also be regarded as an ideal drug carrier.

Other anionic substitutions, such as F^- replacing –OH groups in the whole composition range, resulted in the shrinkage of the *a*-axis and crystal size increasing along the *c*-axis to decrease the solubility of HAP under acidic conditions. Therefore, it has high stability in the biological environment and is more resistant to the corrosion of body fluids.[58,66] The experiments indicated that the higher concentration of fluoride ions in F-HAP would lead to cell stress and cell death using mouse osteoblasts as a model.[67] SiO_4^{4-} can also completely or partially replace PO_4^{3-} to form doped HAP NPs. It has a higher biological activity than pure HAP, attributed to the accelerated dissolution of silicate ions.[68] Drug carriers with different properties were prepared using different ion-doped HAP, which provides a lot of inspiration for the study of HAP materials. There are still many areas about ions and HAP materials waiting for the researchers to test and discover, which will provide more ideas for research. The osteoblast proliferation measurement illustrated that Si-HAP increased osteoblast proliferation by about 1.6 times compared to the undoped HAP.[69] Si-HAP has good biocompatibility and promotes bone formation. A brief summary of the commonly used elemental doping of HAP-based carriers is shown in Table 3.

2.4 Recombination of HAP-based carriers

Sustained release administration is beneficial to reduce the dependence of patients on drugs and frequency of administration, which can increase the drug utilization rate.[70] New biopolymer/inorganic composites have attracted great interest in the field of drug carriers due to their unique structure and properties. The combination of different biopolymers and HAP NPs can achieve the effect of sustained release, stabilization, and/or dispersion of drug particles.[71–73]

Sodium alginate (SA) is a kind of natural polysaccharide, which has been widely used in the food industry and medicine.[74] The *in situ* formation of HAP during the SA sol–gel transition process can slow down the swelling of the SA polymer chain and the drug dissolution rate.[75] Also, it can improve the capture efficiency of drugs and overcome the burst release of diclofenac sodium (DS). Compared with HAP microspheres, the release time of DS was extended to 8 h using SA/HAP drug carriers and prevented the burst release of traditional hydrogel matrix drugs. In addition, HAP combined with polymers can realize the effect of drug-sustained release. Amoxicillin could be released continuously for about 30 days by covering the polymer layer, which is firstly coated with polyvinyl alcohol (PVA) by HAP NPs and then covered with SA (Fig. 4(b)).[76] The release rate of the drug was 51% on the 4th day due to the initial sudden burst and the faster degradation of the external SA. Owing to the slow degradation rate of PVA,[77] the drug maintained sustained release as the time prolonged with 73% on the 10th day and 93% on the 20th day, which significantly achieved the sustained release of drugs.

As for the advantages of reactive functional groups, gel-forming ability, high adsorption capacity, complete biodegradability, bacteriostatic ability, and even anti-tumor ability, chitosan (CS) and its derivatives are biomolecules with great potential.[78] The HAP/CS composite synthesized by ultrasound-assisted sequential precipitation can reduce the burst release

of the model drug.[79] Also, hybrid HAP hollow microparticles can be achieved by combining HAP hollow particles and CS/SA multilayers through layer-by-layer self-assembly.[80] Compared with the solid HAP particles, the high DOX release in the first hour of CS/SA/HAP hollow particles displayed better-sustained release properties with the drug release rate of 28.4% under the same conditions. The PLA-HAP nanofiber carrier prepared by the electrospinning method using hydrophobic polylactic acid (PLA) and biocompatible HAP as raw materials can physically adsorb doxycycline (Doxy) fixed on its surface, achieving slow and stable drug release of Doxy.[81]

To promote aggregation of drug molecules around the target cells, the carrier can also be combined with an antibody, which has high binding specificity with the specific antigen on the surface of the diseased cells to achieve the targeting effect of drug delivery.[82] FA is one of the most widely used targeting agents. DOX@HAP-FA can specifically target folate receptor (FR) overexpressed tumor cells by modifying FA on the surface.[37,83] Under the endocytosis-mediated FA receptor, DOX@HAP-FA nanorods enhanced cellular uptake and further degradation, thereby inhibiting the proliferation of target cells. Hyaluronic acid (HA) can perform tumor targeting effect depending on the specific bind with tumor marker CD44 protein.[84,85] Comparing the targeting of HA/PEI/HAP on cells with different CD44, the cells with more expression of the CD44 receptor will absorb more HA/PEI/HAP NPs (PEI is polyethyleneimine), which can also deliver drugs more effectively and enhance the therapeutic effect. The tumor targeting group DFA_1 can also be transplanted to the surface of HAP NPs.[86] The cellular uptake of drug carriers is enhanced through the binding of DFA_1 and γ-glutamyl transpeptidase (GGT) overexpressed on the cancer cell membrane.

Sometimes, the composite drug carrier has multiple functions in the treatment process. For example, the composite carrier of CaS and HAP can not only be used as the carrier for drug delivery but also contribute to bone regeneration after surgical resection of the tumors in the treatment of osteosarcoma.[87,88] The photoluminescence properties of drug carriers contribute to cell imaging and drug release monitoring in the treatment process. Combining HAP with amino-functionalized carbon quantum dots (CQDs) can enhance the luminescence and UV-vis absorbance of HAP, which is beneficial for imaging in drug delivery applications. In addition, the surface area of HAP can increase from 84.16 $m^2 g^{-1}$ to 129.94 $m^2 g^{-1}$, which is beneficial for drug loading.[89] The study on the synthesis of Mg-HAP samples using the reflux condensation method found that as the concentration of Mg increased, the recombination of charge carriers was blocked, and the photoluminescence intensity increased.[90] The self-luminescent property of Mg-HAP particles, which is because of their surface plasmon, can be used in imaging and drug delivery applications. The composites of HAP and non-functional multiwall carbon nanotubes (MWCNTs) show blue luminescence. But it shows strong white luminescence under UV-vis radiation due to the interaction between Ca^{2+} and carboxyl group in functionalized MWCNT.[91] The relevant studies also showed that the conjugation of carbon nanotubes (CNTs) and graphene nanosheets (GR) can improve the photothermal efficiency of HAP.[92] Under 980 nm near-infrared (NIR) laser irradiation, the photothermal conversion efficiency of CNT/HAP and GR/HAP was 22.2% and 25.9%, respectively. After 7 minutes, the ambient temperature rose to 69.0 °C and 72.2 °C, respectively, which exceeded the tolerance temperature of cancer cells and were enough to induce tumor or cancer cell death. As such, CNT/HAP and GR/HAP are expected to become multimodal platforms to improve the current tumor treatment. The chemical composition changes of the SBF solution were investigated when the complex of graphene oxide (GO) and HAP nanorods was analyzed using inductively coupled plasma optical emission spectrometry.[93] Compared with pure HAP, PEG/GO/HAP released more Ca^{2+} and PO_4^{3-} and showed higher bioactivity.

Except for functional materials and organic polymers, researchers also focussed on the combination of HAP with oxides to realize different functionalization of drug carriers. To avoid cellular toxicity effects, Fe_3O_4 coated with HAP could improve the biocompatibility of Fe_3O_4 and has been used in drug-controlled release systems. At the same time, the compounds of HAP, Fe_3O_4, and ciprofloxacin have shown good biocompatibility and biodegradability, which is beneficial for the treatment of osteomyelitis cases and bone regeneration.[94] Modification with 3-aminopropyl triethoxysilane (APTES) using fructose as a green capping agent[95] can obtain Fe_3O_4/SiO_2/HAP/APTES recombined composite materials with a smaller surface area, pore volume, and pore diameter compared with magnetic Fe_3O_4/SiO_2/HAP. Therefore, it has stronger loading and controlled release ability of drugs than that of pure Fe_3O_4/SiO_2/HAP. As the surface of SiO_2 contains silanol groups, it is conducive to the nucleation and growth of HAP on the surface of SiO_2 in the physiological environment.[96] The results confirmed that SiO_2/HAP samples had better biocompatibility and drug loading ability *in vitro* than SiO_2 samples. Adding a biocompatible HAP microsheet layer to the TiO_2/polymer hybrid layer, can produce a loose film structure and enhance the photocatalytic surface, which can help kill more microorganisms and improve the antibacterial performance.[97] Due to the structure-opening effect of the HAP lamellae, the hybrid film consisting of TiO_2/HAP/polyacrylate (36/24/40 wt%) showed the same antibacterial activity as that with the TiO_2/polyacrylate (60/40 wt%) film. Its excellent antibacterial properties provide a new possibility for the design of drug carriers.

According to the above discussion, there are many preparation methods for HAP-based carriers that can regulate the particle size and surface charge of the carrier to make the carrier easier to be absorbed by cells; it can be doped with different ions to improve its drug-carrying capacity and antibacterial ability. It can be compounded with other materials to obtain the targeting ability. Among them, we should focus on the combination of HAP and different materials, which has been one of the difficulties and hotspots in the field of drug carrier design. Whether HAP is compounded with organic polymers or inorganic materials, all can become excellent drug carriers with special properties. We are sure that there are still many materials waiting to be combined with HAP, and more innovative HAP-based carriers are expected.

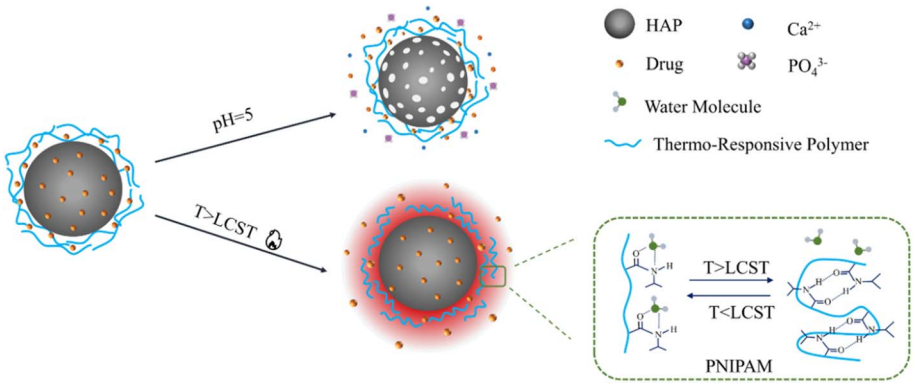

Fig. 5 The pH/thermo response of HAP-based drug carrier.

3. Drug release responsiveness of HAP-based carriers

HAP could be regarded as drug carriers due to their good performance including absorption ability, biocompatibility, nontoxic, biodegradability, and biological activity.[98–100] In addition, HAP combined or compounded with different materials or doped with different ions can gain unexpected functions. As such, the HAP-based carrier can be used to form intelligent drug carriers, which have a controlled drug release response in the tumor microenvironment.[101] With the help of tumor environmental sensitivity, DDS enables drug carriers to release a high concentration of local therapeutic drugs on demand after being stimulated by external stimuli (such as pH value, light irradiation, temperature, and enzyme). It can avoid the premature release of the transported drug before reaching the target tissue and minimize the potential side effects of drugs. This part introduces several kinds of typical responsive nanoscale drug carriers, including pH-responsive, thermal-responsive (Fig. 5), magnetic-responsive, and light-responsive (Fig. 6).

3.1 pH-responsive of drug carrier

The pH of normal tissue is 7.4, while tumor cells use aerobic glycolysis as the central metabolic pathway to produce lactic acid, thus showing stronger acidity.[102] Among various stimulation-responsive DDS, pH-responsive drug carriers have been widely studied due to the pH gradient between tumor cells, inflammatory tissues, and normal cells.

The dissolution rate of HAP would accelerate in an acidic environment.[103] Therefore, drug carriers based on HAP generally show pH responsiveness. Due to the presence of HAP as a coating on the material surface, sodium alginate-hydroxyapatite bilayer-coated iron oxide magnetic nanoparticle composite (SA/HAP/IONP) showed obvious pH sensitivity.[104] When the environmental pH is 5.3, the drug showed a high release rate in the form of diffusion. This means that the pH sensitivity of drug release is improved with the presence of HAP.

In addition, the sulfate-doped HAP nanospheres have a uniform particle size and a highly porous structure.[105] Due to their extremely high surface area and the incorporation of bioactive targeting agents, the DOX-loaded S-HAP/PEG/FA showed sensitive pH response and DOX-triggered release under small changes of pH. Owing to the easy dissolution of HAP in the slightly acidic environment of tumor cells, HAP NPs can be uniformly combined into the silica lattice to enhance their biodegradability.[106] In the acidic environment, the biodegradability of nanoparticles was significantly improved after Ca^{2+} escapes from the skeleton. The nanoparticles obtained from this innovative combination have good biocompatibility, high drug loading efficiency, pH sensitivity, and excellent biodegradability.

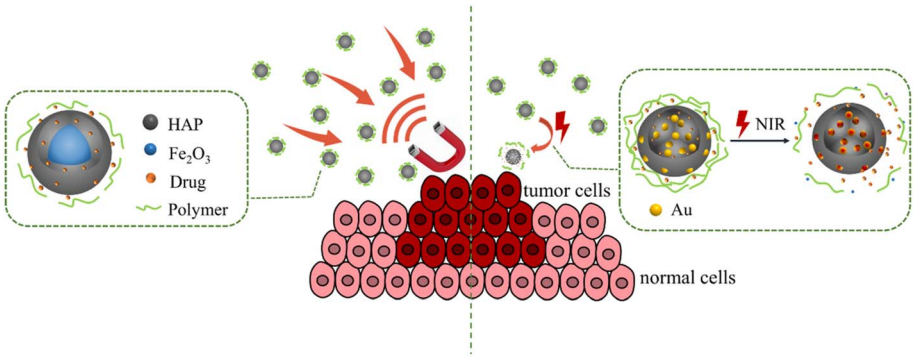

Fig. 6 Magnetic/light response of HAP-based drug carriers.

3.2 Thermo-responsive of drug carrier

Temperature is another potential trigger in various stimuli used in responsive drug delivery systems. Poly-isopropyl acrylamide (PNIPA) is a typical temperature-sensitive polymer that has the hydrophilic hydrophobic transition at the lower critical solution temperature (LCST) of about 32 °C.[107] When the temperature is below LCST, the drug is locked in the carrier's structure. When the temperature was increased, the PNIPA chain became hydrophobic and shrunk, allowing the drug to be released.[108] It was found that the drug release rate of poly (*N*-isopropyl acrylamide) HAP composite (PNIPAM-*m*-HAP) microspheres at 37 °C was faster than that at 25 °C, which shows obvious thermo-sensitivity. In addition, the poly(*N*-isopropylacrylamide acrylic acid copolymer) (PNA) obtained by modifying PNIPAM with acrylic acid showed excellent response to temperature and pH changes, which can be used as an intelligent polymer cap to control the drug delivery of hybrid nanoparticles.[109] Au/SiO_2/HAP nanocarriers can be modified with PNA to obtain a multi-response for the remote control of drug delivery. When the environmental pH was 4.5, the drug release rates of Au/SiO_2/HAP at 25 °C and 40 °C within 48 hours were 69.8% and 81.3%, respectively, performing sensitive thermal response.[110] The composite combined with an intelligent polymer with a hybrid inorganic skeleton, which provided a simple method for the preparation of multi-response drug carriers with good biocompatibility and degradability.

Furthermore, the expansion of nanoparticles at higher temperatures leads to the decrease of matrix density, which is conducive to the escape of drugs and improves the diffusion rate of drugs. The analysis of drug release from the hydroxyapatite gelatin polymer composite (GEL/HAP) at a pH of 4 with various temperatures of 32 °C, 37 °C, and 42 °C showed that the initial burst release rates were 5%, 35%, and 50%, respectively, which increased with the increase of temperature.[111] It can be used to design drug carriers with better sustained-release and thermal response.

3.3 Magnetic response of drug carrier

In addition to using the internal stimulation of acidity and temperature to activate the drug carrier *in vivo*, researchers have also tried to combine functional materials with inorganic nanomaterials to enable them to release drugs under external stimulation. The advantage of an external responsive nanocarrier is that the drug release can be turned on or off as needed, which may make it possible for clinicians to remotely activate external stimuli for disease treatment.

Magnetic response DDS had a wide application in the target drug delivery, which is realized by external magnetic guidance of electromagnetic coils or various permanent magnets.[112,113] Magnetic HAP drug carriers can be prepared by adding paramagnetic, ferromagnetic, or superparamagnetic materials. Among them, superparamagnetic iron oxide nanoparticles (SPIONs) obtained low remanence and coercivity to prevent caking, which is conducive to maintaining long-term circulation in the body.[114] The combination of HAP nanorods and superparamagnetic Fe_3O_4 nanoparticles can form a dual-phase Fe_3O_4/HAP composite with high saturation magnetization of 18 emu g^{-1}.[115] Due to their low coercivity, large specific surface area, high mesoporous volume, and good magnetism, Fe_3O_4/HAP composites are suitable for targeted DDS. In addition, andrographolide loaded on the Fe_3O_4/HAP nanocomposite showed high antiproliferative activities and the induction of apoptosis against the A431 cell lines with rapid time. Fe_3O_4/HAP nanocomposites could decrease drug delivery time and dosage and reduce cancer pain.

A novel magnetic HAP-based carrier based on carbon nanotubes/hydroxyapatite composite (CNT (Fe)/HAP) was prepared by *in situ* synthesis of carbon nanotubes in HAP nanopowder using an iron catalyst with the average DOX load of 130%.[116] In addition, the saturation magnetization, coercivity, and saturation magnetization ratio of DOX@FA/CNT (Fe)/HAP were 0.88 emu/g, 668.96 Oe, and 0.44, respectively. It showed that DOX@FA/CNT (Fe)/HAP can be used to transport drugs under strong external magnetic fields and realize the magnetically targeted drug delivery. HAP NPs doped with strontium have excellent antibacterial properties, which are suitable for targeted anticancer drug delivery after doping iron ions.[117] Relevant literature pointed out that the prepared Sr-HAP and Sr, Fe-HAP NPs were in the form of nanowhiskers and nanorods, respectively, showing paramagnetism and superparamagnetism, respectively. Due to its superparamagnetism, Sr, Fe-HAP nanorods have a good response to the magnetic field. In addition, the $CoFe_2O_4$/HAP composite drug carrier with a core–shell structure is a new type of biomedicine magnetic material, which has aroused the interest of researchers.[118] $CoFe_2O_4$ is encapsulated in rod-shaped HAP, forming a composite material with a saturation magnetization of 9.04 emu g^{-1} and a coercivity of 1000 T. The synthesized $CoFe_2O_4$/HAP composite drug carrier showed ferromagnetic properties at room temperature and that the saturation magnetization can be

Table 4 The summary of HAP-based carriers with magnetic responsiveness

Carrier	Size (nm)	Morphology	Drug	Saturation magnetization (emu g^{-1})	Coercivity (Oe)	Ref
Fe_3O_4/HAP	80	Nanorods	—	18.2	0.09	115
CNT (Fe)/HAP	400–600	Rod-shaped	DOX	4.17	427.57	116
Sr, Fe-HAP	120	Rod-shaped	DOX	4.3	—	117
$CoFe_2O_4$/HAP	50	Spherical	Ibuprofen	18.3	100	119
$CuFe_{12}O_{19}$@HAP-APTES	73	Spherical	Atenolol	9.2	—	120

further enhanced by heat treatment.[119] Alternatively, $CuFe_{12}O_{19}$@HAP magnetic nanocomposites can be synthesized using the ultrasound-assisted precipitation method and functionalized using APTES, where the amine groups in APTES can bind to atenolol drugs to increase the drug loading. $CuFe_{12}O_{19}$@HAP-APTES nanoparticles have good magnetic responsiveness with saturation magnetization of 9.2 emu g^{-1}.[120] Currently, a part of the composite magnetic HAP NPs based drug carriers have been successfully used in biomedical applications (Table 4), including bio-imaging and drug delivery.[121]

3.4 Light response of drug carrier

Light stimulation is also a useful method to trigger drug release. The advantages of using light as a stimulus lie in its easy application, low toxicity to the body, and more accurate focus on the target tissue. More importantly, it can combine chemotherapy with NIR-mediated photothermal therapy (PTT), which has a better ablation effect on tumors.[122] The intelligent layered composite hollow drug carrier prepared by polyelectrolyte, inorganic particles, and metal nanoparticles have good light response performance. Drug-loaded nanoparticles have a hollow HAP as the core, a multilayer polymer, and gold nanoparticles as a shell.[123] Under the irradiation of a NIR laser, Au NPs can be rapidly heated causing partial collapse of the polyelectrolyte multilayer and the rapid release of DOX. In addition, Au/SiO_2/HAP showed a high release amount and the cumulative DOX release amount increased to 55.95% within 12 h at pH 4.5, while that of Au/SiO_2 was only 30.76% at the same condition.[124] Moreover, Au/SiO_2/HAP displayed a high drug load of 98.89%, and the drug can be released slowly and continuously. It exhibited excellent NIR- and pH-responsive drug-release properties due to the NIR-responsiveness of Au NRs and pH-responsiveness of HAP in acid media, respectively. The prepared hybrid nanoparticles displayed great potential in controllable drug delivery areas owing to their high drug-loading efficiency, excellent pH/NIR sensitivity, and biodegradability. HAP can be self-assembled *in situ* around Ti_3C_2@AuNRs and then combined with polydopamine (PDA) to prepare Ti_3C_2@AuNRs/HAP/PDA nanocomposites. The strong near-infrared absorption ability of Ti_3C_2@AuNRs enables the composite material to have a significant photothermal conversion efficiency (38.6%). The negative charges on the surface of HAP and the adhesion of PDA make the composite material exhibit good drug loading capacity (88.3%) for DOX. Ti_3C_2@AuNRs/HAP/PDA has NIR- and pH-responsive drug release behavior,[125] which has great application prospects in remote-controlled drug delivery and photothermal therapy fields.

HAP nanorods were combined with monolayer GO to form a GO/HAP composite drug carrier with high DOX loading of 698.7 μg mg^{-1} and photothermal conversion performance.[126] Its drug release performance is controlled by pH and NIR. The unique acidic environment at the tumor site and the heat energy brought by NIR are conducive to the release of DOX, which can achieve the effect of targeted drug delivery. Cu/F-HAP hollow microspheres coated with PDA can be prepared by the impregnation method due to the strong near-infrared absorption and high photothermal conversion efficiency of polydopamine (PDA). PDA can bind well with HAP through Ca–O and O–H bonds. Under the 808 nm near-infrared laser, the sample temperature increased by about 10 °C within 12 minutes, demonstrating excellent photothermal conversion efficiency and good photothermal stability after five cycles.[127] *In vitro* tumor treatment research showed that the combined therapy has a better synergistic therapeutic effect than simple chemotherapy or PTT, which demonstrated great application potential of HAP-based nanocomposites in tumor treatment.

4. Drug loading method

Currently, adsorption after carrier synthesis (physical adsorption or chemical adsorption) or *in situ* loading during carrier synthesis are the main ways to load drugs onto the carrier (Fig. 7). In the adsorption process, carrier preparation is an

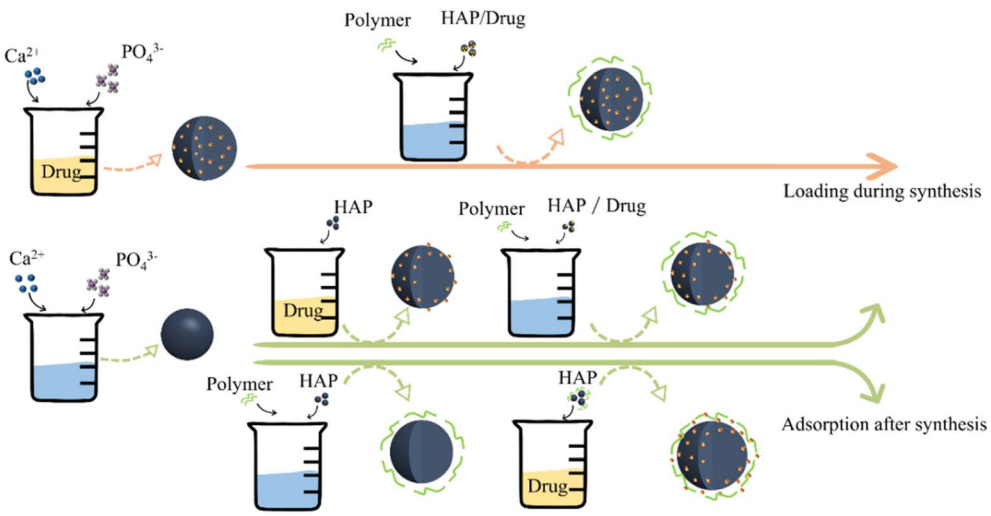

Fig. 7 Drug loading through adsorption and *in situ* methods.

independent step, which can optimize the properties of the carrier in a variety of ways, such as doping, modification, and recombination. The adsorption forms include the physical adsorption of drugs (carrier pores and surface) and covalent grafting. Different from the traditional drug adsorption loading on the pre-synthetic carrier, *in situ* loading mainly adds the drug into the calcium or phosphate solution during the preparation of HAP. The drug is wrapped in the carrier to realize encapsulation instead of increasing the load on the carrier preparation.

4.1 Drug-adsorption loading

Drug-adsorption loading is the most commonly used drug-loading method. The carrier is added to the solution containing drug molecules and soaked for a while under certain conditions (*e.g.*, heating, stirring, and ultrasonic). Many researchers studied the adsorption and release process of different drugs on HAP and speculated the availability of materials according to the predictability of the adsorption model.[128] HAP NPs are commonly modified before the drug loading to improve the adsorption capacity. The interaction between Ca^{2+} on the surface of HAP and carbonyl (–O) on the drug was the main reason for the adsorption. The length of the Ca–O bond shortened as a consequence of Zn-doping, which indicated that strong interaction existed between DOX and the surface of Zn-HAP.[129] Compared with pure HAP, the doping ions can improve the specific surface area and zeta potential to enhance the binding energy between DOX and HAP, which is conducive to improving the DOX loading capacity and sustained release time. In addition, the doping of Al^{3+}, Mg^{2+}, and Sr^{2+} plasma can also improve the drug loading of HAP. Therefore, it is of great significance to select appropriate doping ions to promote the study of HAP as a drug carrier.

HAP modified with special functional groups can also improve drug adsorption. For example, the inner surface of HAP NPs was functionalized with (3-aminopropyl)trimethox-ysilane (APTS).[130] Compared with pure HAP, amino-functionalized carriers have higher drug adsorption capacity and slower drug release rate. The advantage of the adsorption drug loading method is that it is easy to operate, but the drug may be released suddenly, which may affect the therapeutic effect.

It is known that organic or inorganic materials can be used as templates to regulate the porous or hollow structure of HAP, which can greatly improve the drug loading rate. Due to the wide variety of materials that can be used as template and coating agents, the template preparation method has become the most effective method to improve drug loading and is also the worthiest of further exploration. In addition to being used as templates, some polymers can also be used to modify the carrier after drug adsorption, which can significantly improve the sustained release effect of the drug carrier. For example, DOX was adsorbed on the synthesized HAP NPs used as filling materials, and then coated on the surface with CS.[131] Compared with DOX@HAP, the drug release rate of DOX@HAP/CS is slower. The structure design of the drug-loading method with sandwich lamination has gradually been more widely applied and investigated.

4.2 *In situ* loading during synthesis

In situ drug loading mainly involves adding drugs to calcium or phosphate solution during the process of preparing HAP. The drug is encapsulated in a carrier during the preparation process. The characteristics of the drug affect the encapsulation effect. For different drugs, the carrier may show different loading and release effects. Drug loading can occur simultaneously with the formation of calcium phosphate (CPs) nanocarriers in the same reaction system.[132] Large numbers of CPs clusters with ultrahigh specific surface area form at the early stage of the precipitation reaction, providing many binding sites for the drug molecules. During the formation of HAP nanocarriers, the *in situ* drug molecules can be adsorbed on the surface of CPs clusters without any surfactant. The synthesis of nano-carriers and subsequent drug loading is completed in one step, which avoids the post-processing that may inactivate the drug molecule binding sites.

The simulated drug R6G was mixed with $CaCl_2$ solution, then sodium alginate and Na_2HPO_4 solutions were added to form SA/HAP with a core–shell structure.[133] In the process of HAP synthesis, drug encapsulation effectively improved the drug loading capacity of the carrier, and the presence of positively charged R6G improved the synthesis efficiency of HAP. Since the positively charged R6G molecules need to diffuse from the HAP core, the burst release of the drug was avoided in the initial stage, showing a good sustained-release effect. The relevant research report that adding DS to the aqueous solution containing SA and $(NH_4)_2HPO_4$ and then dropping the solution into $Ca(NO_3)_2 \cdot 4H_2O$ aqueous solution using a hypodermic syringe to immediately formed a milky white drug-loaded SA/HAP beads.[75] The encapsulation efficiency and release rate of DS are obviously improved using this synthesis method.

In situ drug loading has greater advantages in drug loading and release rates and can seal the drug more stably in the carrier. However, it is necessary to consider the physical and chemical properties of drugs, which affect the formation of HAP during the synthesis process, such as drug solubility and drug particle size. The high requirements of the drug limit the expanded application of the *in situ* drug delivery during drug carrier preparation. By comparison, the method of loading drugs after carrier synthesis could overcome the defects of drug properties based on the simpler principle. The anionic groups on the drug surface were easily absorbed by HAP. However, the burst release of the drug during the desorption process is unavoidable, which is unfavorable to realizing the sustained release effect. In short, the selection of drug-loading methods should take into account the application limitations and drug properties.

5. Properties of HAP-based carriers

In the slightly acidic environment, HAP particles would dissolve to release Ca^{2+} and PO_4^{3-}, which could be swallowed or absorbed by cells *in vivo* or discharged with body fluid.[134] In addition, the acid-soluble properties of HAP are conducive to the degradation and release of drugs in the weak acidic environment of

the tumor, which has great potential for the delivery of tumor drugs. Due to their nontoxic and biocompatibility, HAP NPs have become the preferred material in the field of drug carriers.

5.1 Effect of the carrier on drug efficacy

As drug carriers, HAP NPs can achieve targeted delivery and improve the drug treatment effect. To reduce the frequency of administration, increase patient compliance, or reduce the side effects of drugs, the drug carriers are designed to achieve the sustained release effect. Coating biopolymer on the HAP surface is the most efficient method to achieve the drug's sustainable release. The drug is locked on a HAP-based composited drug carrier and then slowly released with the degradation after being affected by the tumor microenvironment. Due to the unique properties of HAP (high solubility in an acidic environment), it is equivalent to the second lock on the drug. Therefore, HAP is an excellent material for the preparation of drug sustained-release carriers, which is conducive to promoting the absorption of drugs *in vivo* and improving the efficacy of drugs for the human body.

Compared with free collagen and ovalbumin, using HAP as a protein carrier is more easily absorbed by bone tissue.[135,136] Similarly, compared with free DOX, DOX@HAP/ZnO/F127/FA has higher cellular uptake efficiency.[137] In addition, conjugated FA and UVA irradiation on the surface of nanocomposites provide dual targeting and produce *in situ* reactive oxygen species, which provide the expected toxicity in conjugation and improve the efficiency of photodynamic therapy. In comparison, the drug delivery system using HAP/GO as a drug carrier with lower content of DOX and higher DOX performed the same cancer cell death rate, indicating the synergistic therapy of the nanocomposites in the cell viability measurements.[126]

Excessive Ca^{2+} produced after HAP dissolution will lead to cell calcification and death. This is the reason why HAP has antitumor properties. With polyglutamic acid (PGA) as the coordination agent, PGA/HAP are easy to assemble into spherical nanoclusters with low crystallinity.[138] The good dispersion and solubility of PGA/HAP in the tumor environment improved its internalization, which significantly increased the intracellular calcium influx by about 40%. Under the synergistic action of DOX and calcium overload, the hybrid system selectively enhanced the toxicity to tumor cells. *In vivo* experiments further confirmed that the system has higher selective tumor inhibition and reduced cardiotoxicity, which is an effective anti-tumor platform. PAA is also used as a coordination agent. The surface of the synthesized composite particles is rich in carboxyl groups, which promote the internalization of particle cells. Due to the low crystallinity of calcium phosphate, Ca^{2+} is gradually released through dissolution. The prepared composite nanomaterials can increase the cytoplasmic calcium content of tumor cells by 175% and further inhibit the activity of tumor cells by more than 80%.[37]

5.2 Reduce the side effects of drugs

In the treatment of some chronic diseases or cancers, the drugs cannot selectively target the affected areas, which may cause serious side effects to normal tissues, and due to the short biological half-life and poor bioavailability, high doses and frequent administration are required. However, the HAP-based carrier has excellent biocompatibility, biodegradability, and targetability, which is safer for the body than other materials. Loading drugs with this new system can reduce drug side effects and is safer than free drugs. It can improve the treatment efficiency of pathological tissue and reduce the toxic and side effects on other tissues (Fig. 8).

DOX has broad-spectrum antitumor activity, such as in leukemia, lymphoma, and solid tumors. However, it has severe side effects, including low selectivity and dose-dependent cardiotoxicity.[139,140] The –OH and carbonate groups on HAP crystals can form strong hydrogen bond interactions with –OH and $–NH_2$ groups in DOX, which enables their DOX to be stably loaded on HAP supports. DOX loaded on HAP-based carriers can greatly reduce its cardiotoxicity and cytotoxicity.[141] In addition, the modification of HAP by other materials can be used to enhance the targeting. The DOX@HAP/MOF/Fe_3O_4/Fe nanocomposite microspheres produced good saturation magnetization and pH response characteristics, which could control the release of DOX loaded on the drug carrier in the

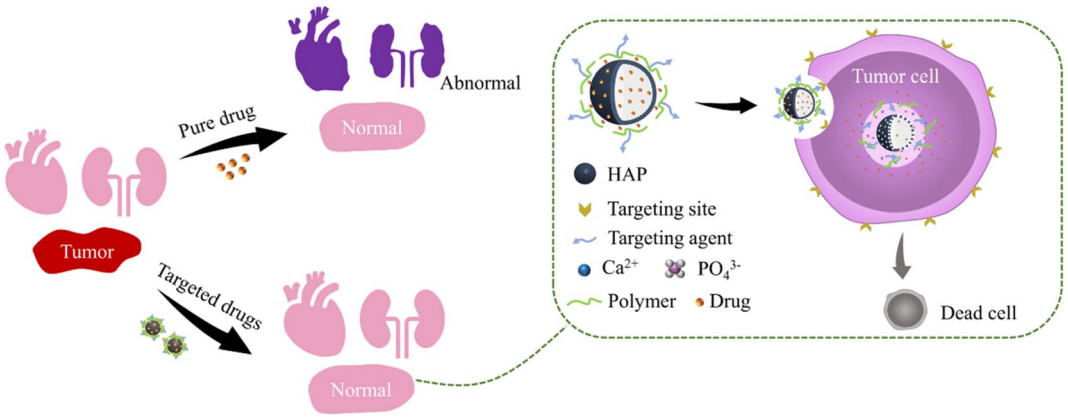

Fig. 8 HAP-based targeted carriers reduce drug side effects.

simulated acidic tumor cell environment to effectively kill tumor cells and reduce the toxic side effects on normal tissue.[142]

The anticancer drug cisplatin is also widely used in tumor treatments because of its powerful therapeutic effect. However, cisplatin is a highly accumulative drug, which is prone to nephrotoxicity and serious side effects. The HAP drug carrier loaded with cisplatin of suitable dimensions accumulates at the tumor site based on the enhanced permeability and retention effect by intravenous injection. The acidic environment of tumor tissues may favor the dissolution of HAP and the release of the Pt complexes, which can effectively avoid the damage of cisplatin to other healthy tissues.[143] HAP bone cement-containing cisplatin was implanted into rabbit bone for local chemotherapy to maintain a high concentration of anticancer drugs locally. It could promote the growth of new bone after tumor resection, increase the mechanical strength of fragile bone, reduce the side effects of cisplatin and damage to other parts, and increase the action time and drug efficacy of cisplatin in the affected area.[144] Cisplatin was implanted into normal back muscle, tibia, and experimental tumors of mice through a porous HAP carrier.[145] The diffusion rate of cisplatin in blood and other organs (liver, kidney, and brain) was less than 10% of the implanted site and released uniformly for more than 3 months. It proved that HAP carriers could reduce the toxic and side effects of cisplatin on normal tissues.

5.3 Effect of the carrier on the organism

As for normal tissues, the synthetic HAP-based drug carriers perform good bone induction. Compared with allogeneic bone and bone grafts, HAP-based drug carriers usually bind well to the surrounding host bone and promote the formation of new bone, combine with new bone, and recover the damaged bone tissue.[146]

Dexamethasone (DEX)-loaded polylactic acid-glycolic acid (PLGA) microspheres were immobilized on the surface of HAP scaffolds. This composite HAP scaffold can enhance bone regeneration *in vivo*.[147] HAP nanocrystals are also considered to be important bioactive components to promote cartilage regeneration.[148] Compared with PLGA scaffolds, HAP NPs can significantly promote the adhesion and proliferation of chondrocytes and have better cartilage regeneration ability without using any growth factors or gene transfer.[149] This may be due to its biocompatibility, which is similar to the minerals of natural bone tissue from chemical and structural points of view. The prepared highly interconnected microporous HAP bio-ceramic scaffolds have the surface morphology of nanosheets, nanorods, and micro-nano mixtures (a mixture of nanorods and micro rods).[150] HAP bio-ceramics with these micro/nano morphologies can significantly enhance cell attachment, cell viability, alkaline phosphatase (ALP) activity, and mRNA expression of osteogenic-related genes of rat bone marrow stromal cells (bMSCs). When HAP delivers drugs to bone tissue, it usually acts as a scaffold or template together with implants to induce immature cells and stimulate these cells to develop into mature osteoblasts. HAP surface features support osteoblast adhesion and differentiation and promote bone growth by slowly replacing the adjacent living bone by guiding the newly formed bone on its surface or down into pores, pipes, or channels.[151,152]

In addition, HAP can also activate fibroblasts and accumulate vascular endothelial cells, to support the healing of skin wounds. Electrodeposited HAP (pHA) powder was added to silk fibroin (SF) and applied to full-thickness skin wounds in pigs.[153] The study found that pHA-containing SF gel had a higher promotion effect on wound healing, re-epithelialization, and matrix formation compared to other gel complexes prepared in that study. Therefore, the application of HAP as a drug carrier can not only achieve sustained release, targeting, and other effects but it may also promote the recovery of the damaged tissues.

Although HAP is chemically similar to bone minerals, this does not mean that they are completely harmless to the body. Calcium phosphate crystals can induce the release of proinflammatory cytokines. Smaller calcium phosphate crystals can disrupt the stability of atherosclerotic plaques by triggering inflammation and leading to the death of vascular smooth muscle cells.[154,155] The reason for the toxicity of NPs is unknown in most cases.[156,157] This may be due to its special characteristics, such as the high specific surface area of NPs or its surface chemical properties. When macrophages were exposed to gel HAP NPs, colloidal HAP NPs, or HAP NPs after spray drying, cell death occurred.[158] Among them, the gel state of HAP showed the greatest toxicity, and the cytotoxicity of nanoparticles after spray drying was greatly reduced. This is because the degree of cytotoxicity to cells is closely related to the degree of HAP uptake by cells. The main cause of cell toxicity of HAP may be related to the release of Ca^{2+}. Therefore, controlling the large intake of HAP NPs can avoid the possible adverse effects of Ca^{2+} on the body.

6. Conclusions and perspectives

HAP has been widely used in chemistry, biology, and medicine due to its biocompatibility, biodegradability, and bioactivity. This review discusses various synthesis methods to modify HAP for improving the drug loading capacity. The main responsiveness mechanism of drug release in tumor therapy is also emphasized, including microenvironment *in vivo* and external stimulation. Modified HAP-based drugs carried by doping or recombination showed high sensitivity to the environment and achieve the targeted drug releases. In addition, the drug could remain on the HAP-based composite carrier and then be sustainably released with the degradation of biopolymer to promote the absorption of drugs and improve the drug efficacy of tumor treatment. HAP-based drug carriers with various targeting types are suitable for corresponding drug delivery systems (cardiovascular system, respiratory system, digestive system, blood system, immune system, and so on), which need further systematic research and delicate classification. Above all, HAP-based drug carriers can be expected to be one of the most effective carriers for drug delivery.

Conflicts of interest

There are no conflicts to declare.

Acknowledgements

The author thanks the students of this research group for their efforts in collecting some literature data and mapping.

References

1 C. L. Chaffer and R. A. Weinberg, *Science*, 2011, **331**, 1559–1564.
2 N. Behranvand, F. Nasri, R. Zolfaghari Emameh, P. Khani, A. Hosseini, J. Garssen and R. Falak, *Cancer Immunol., Immunother.*, 2022, **71**, 507–526.
3 L. Yang, Q. Ning and S. S. Tang, *J. Immunol. Res.*, 2022, **2022**, 8052212.
4 V. P. Torchilin, *Eur. J. Pharm. Sci.*, 2000, **11**, S81–S91.
5 S. Raveendran, A. K. Rochani, T. Maekawa and D. S. Kumar, *Materials*, 2017, **10**.
6 V. (Gajre) Kulkarni, K. Butte and S. Rathod, *Research Gate*, 2012, **3**, 1597–1613.
7 N. Minocha and V. Kumar, *Mater. Today: Proc.*, 2022, **69**, 614–619.
8 S. K. Hari, A. Gauba, N. Shrivastava, R. M. Tripathi, S. K. Jain and A. K. Pandey, *Drug Delivery Transl. Res.*, 2023, **13**, 135–163.
9 A. K. Sharma, A. Gothwal, P. Kesharwani, H. Alsaab, A. K. Iyer and U. Gupta, *Drug Discovery Today*, 2017, **22**, 314–326.
10 M.-X. Zhao, E.-Z. Zeng and B.-J. Zhu, *ChemNanoMat*, 2015, **1**, 82–91.
11 M. I. Kay, R. A. Young and A. S. Posner, *Nature*, 1964, **204**, 1050–1052.
12 M. Sadat-Shojai, M. Atai, A. Nodehi and L. N. Khanlar, *Dent. Mater.*, 2010, **26**, 471–482.
13 I. Ratha, P. Datta, V. K. Balla, S. K. Nandi and B. Kundu, *Ceram. Int.*, 2021, **47**, 4426–4445.
14 A. Lucia de Souza Niero, N. M. Possolli, D. Floriano da Silva, K. B. Demétrio, J. J. Zocche, G. M. Soares de Souza, J. F. Dias, J. L. Vieira, J. D. Viana Barbosa, M. B. Pereira Soares, O. R. Klegues Montedo and S. Arcaro, *Ceram. Int.*, 2023, DOI: **10.1016/j.ceramint.2023.05.068**.
15 M. N. Obaid, O. H. Sabr and A. A. Hussein, *J. Achiev. Mater. Manuf. Eng.*, 2021, **1**, 21–30.
16 M. C. Lee, H. Seonwoo, K. J. Jang, S. Pandey, J. Lim, S. Park, J. E. Kim, Y.-H. Choung, P. Garg and J. H. Chung, *Bioact. Mater.*, 2021, **6**, 2742–2751.
17 W. Xiao, H. Fu, M. N. Rahaman, Y. Liu and B. S. Bal, *Acta Biomater.*, 2013, **9**, 8374–8383.
18 F. Fayyazbakhsh, M. Solati-Hashjin, A. Keshtkar, M. A. Shokrgozar, M. M. Dehghan and B. Larijani, *Colloids Surf., B*, 2017, **158**, 697–708.
19 D. Luo, X. Xu, M. Z. Iqbal, Q. Zhao, R. Zhao, J. Farheen, Q. Zhang, P. Zhang and X. Kong, *Pharmaceutics*, 2021, **13**, 1428.
20 Y. Sun, Y. Chen, X. Ma, Y. Yuan, C. Liu, J. Kohn and J. Qian, *ACS Appl. Mater. Interfaces*, 2016, **8**, 25680–25690.
21 N. A. S. Mohd Pu'ad, P. Koshy, H. Z. Abdullah, M. I. Idris and T. C. Lee, *Heliyon*, 2019, **5**, e01588.
22 W. Liu, G. Qian, L. Liu, B. Zhang and X. Fan, *Mater. Lett.*, 2018, **217**, 177–180.
23 J. M. Coelho, J. A. Moreira, A. Almeida and F. J. Monteiro, *J. Mater. Sci.: Mater. Med.*, 2010, **21**, 2543–2549.
24 M. Yoshimura, H. Suda, K. Okamoto and K. Ioku, *J. Mater. Sci.*, 1994, **29**, 3399–3402.
25 S. C. Cox, R. I. Walton and K. K. Mallick, *Bioinspired, Biomimetic Nanobiomater.*, 2015, **4**, 37–47.
26 B. Szczęśniak, S. Borysiuk, J. Choma and M. Jaroniec, *Mater. Horiz.*, 2020, **7**, 1457–1473.
27 M. Parashar, V. K. Shukla and R. Singh, *J. Mater. Sci.: Mater. Electron.*, 2020, **31**, 3729–3749.
28 A. Mariappan, P. Pandi, R. Rajeswarapalanichamy, K. Neyvasagam, S. Sureshkumar, M. K. Gatasheh and A. A. Hatamleh, *Environ. Res.*, 2022, **211**, 113079.
29 A. Afshar, M. Ghorbani, N. Ehsani, M. R. Saeri and C. C. Sorrell, *Mater. Des.*, 2003, **24**, 197–202.
30 M. Aizawa, A. E. Porter, S. M. Best and W. Bonfield, *Biomaterials*, 2005, **26**, 3427–3433.
31 M. Aizawa, H. Ueno, K. Itatani and I. Okada, *J. Eur. Ceram. Soc.*, 2006, **26**, 501–507.
32 G. Zhang, J. Chen, S. Yang, Q. Yu, Z. Wang and Q. Zhang, *Mater. Lett.*, 2011, **65**, 572–574.
33 K. Ioku, G. Kawachi, S. Sasaki, H. Fujimori and S. Goto, *J. Mater. Sci.*, 2006, **41**, 1341–1344.
34 R. Zhu, R. Yu, J. Yao, D. Wang and J. Ke, *J. Alloys Compd.*, 2008, **457**, 555–559.
35 F. Ghorbani, A. Zamanian, A. Behnamghader and M. D. Joupari, *Mater. Sci. Eng., C*, 2019, **94**, 729–739.
36 G. Qian, W. Liu, L. Zheng and L. Liu, *Results Phys.*, 2017, **7**, 1623–1627.
37 S. Zhang, X. Ma, D. Sha, J. Qian, Y. Yuan and C. Liu, *J. Mater. Chem. B*, 2020, **8**, 9589–9600.
38 W. Zhang, Y. Chai, X. Xu, Y. Wang and N. Cao, *Appl. Surf. Sci.*, 2014, **322**, 71–77.
39 X. Huang, L. Li, T. Liu, N. Hao, H. Liu, D. Chen and F. Tang, *ACS Nano*, 2011, **5**, 5390–5399.
40 X. Xia, J. Chen, J. Shen, D. Huang, P. Duan and G. Zou, *Adv. Powder Technol.*, 2018, **29**, 1562–1570.
41 H. Chen and S. Leng, *Ceram. Int.*, 2015, **41**, 2209–2213.
42 S. Mondal, G. Hoang, P. Manivasagan, H. Kim and J. Oh, *Ceram. Int.*, 2019, **45**, 17081–17093.
43 M. Y. Ma, Y. J. Zhu, L. Li and S. W. Cao, *J. Mater. Chem.*, 2008, **18**, 2722–2727.
44 Z. L. Liu, Q. Y. Jia, X. D. Li, S. P. Li, J. Shen, J. Lin and D. X. Li, *Colloids Surf., A*, 2020, **586**, 124231.
45 M. Mabrouk, R. Rajendran, I. E. Soliman, M. M. Ashour, H. H. Beherei, K. M. Tohamy, S. Thomas, N. Kalarikkal, G. Arthanareeswaran and D. B. Das, *Pharmaceutics*, 2019, **11**, 294.
46 L. Chen, J. M. McCrate, J. C. Lee and H. Li, *Nanotechnology*, 2011, **22**, 105708.

47 G. Yin, Z. Liu, J. Zhan, F. Ding and N. Yuan, *Chem. Eng. J.*, 2002, **87**, 181–186.
48 S. Dasgupta, A. Bandyopadhyay and S. Bose, *Acta Biomater.*, 2009, **5**, 3112–3121.
49 B. Palazzo, M. Iafisco, M. Laforgia, N. Margiotta, G. Natile, C. L. Bianchi, D. Walsh, S. Mann and N. Roveri, *Adv. Funct. Mater.*, 2007, **17**, 2180–2188.
50 G. D. Venkatasubbu, S. Ramasamy, G. S. Avadhani, V. Ramakrishnan and J. Kumar, *Powder Technol.*, 2013, **235**, 437–442.
51 L. G. Bach, M. R. Islam, T. S. Vo, S. K. Kim and K. T. Lim, *J. Colloid Interface Sci.*, 2013, **394**, 132–140.
52 D. Li, Y. Zhu and Z. Liang, *Mater. Res. Bull.*, 2013, **48**, 2201–2204.
53 C. R. Gautam, S. Kumar, S. Biradar, S. Jose and V. K. Mishra, *RSC Adv.*, 2016, **6**, 67565–67574.
54 X. Jiang, Y. Zhao, C. Wang, R. Sun and Y. Tang, *Mater. Chem. Phys.*, 2022, **276**, 125440.
55 Q. Fan, F. Fan, W. Xu, H. Zhang and N. Liu, *J. Alloys Compd.*, 2021, **879**, 160414.
56 E. Landi, G. Logroscino, L. Proietti, A. Tampieri, M. Sandri and S. Sprio, *J. Mater. Sci.: Mater. Med.*, 2008, **19**, 239–247.
57 I. V. Fadeev, L. I. Shvorneva, S. M. Barinov and V. P. Orlovskii, *Inorg. Mater.*, 2003, **39**, 947–950.
58 S.-J. Kim, H.-G. Bang, J.-H. Song and S.-Y. Park, *Ceram. Int.*, 2009, **35**, 1647–1650.
59 Y. Xu, L. An, L. Chen, H. Xu, D. Zeng and G. Wang, *Adv. Powder Technol.*, 2018, **29**, 1042–1048.
60 A. Pal, P. Nasker, S. Paul, A. Roy Chowdhury, A. Sinha and M. Das, *J. Mech. Behav. Biomed. Mater.*, 2019, **90**, 328–336.
61 E. Murugan and C. R. Akshata, *Colloids Surf., B*, 2022, **219**, 112822.
62 T. N. Kim, Q. L. Feng, J. O. Kim, J. Wu, H. Wang, G. C. Chen and F. Z. Cui, *J. Mater. Sci.: Mater. Med.*, 1998, **9**, 129–134.
63 Q. Zhou, T. Wang, C. Wang, Z. Wang, Y. Yang, P. Li, R. Cai, M. Sun, H. Yuan and L. Nie, *Colloids Surf., A*, 2020, **585**, 124081.
64 H. Kim, S. Mondal, B. Jang, P. Manivasagan, M. S. Moorthy and J. Oh, *Ceram. Int.*, 2018, **44**, 20490–20500.
65 A. Turlybekuly, A. D. Pogrebnjak, L. F. Sukhodub, L. B. Sukhodub, A. S. Kistaubayeva, I. S. Savitskaya, D. H. Shokatayeva, O. V. Bondar, Z. K. Shaimardanov, S. V. Plotnikov, B. H. Shaimardanova and I. Digel, *Mater. Sci. Eng., C*, 2019, **104**, 109965.
66 E. Bertoni, A. Bigi, G. Cojazzi, M. Gandol, S. Panzavolta and N. Roveri, *J. Inorg. Biochem.*, 1998, **72**, 29–35.
67 P. Nasker, M. Mukherjee, S. Kant, S. Tripathy, A. Sinha and M. Das, *Ceram. Int.*, 2018, **44**, 22008–22013.
68 A. E. Porter, C. M. Botelho, M. A. Lopes, J. D. Santos, S. M. Best and W. Bonfield, *J. Biomed. Mater. Res., Part A*, 2004, **69**, 670–679.
69 T. Sun, M. Wang, Y. Shao, L. Wang and Y. Zhu, *Biol. Trace Elem. Res.*, 2018, **181**, 82–94.
70 J. V. Natarajan, C. Nugraha, X. W. Ng and S. Venkatraman, *J. Controlled Release*, 2014, **193**, 122–138.
71 L. Gritsch, M. Maqbool, V. Mourino, F. E. Ciraldo, M. Cresswell, P. R. Jackson, C. Lovell and A. R. Boccaccini, *J. Mater. Chem. B*, 2019, **7**, 6109–6124.
72 A. K. Nayak, M. S. Hasnain, S. S. Nanda and D. K. Yi, *Curr. Pharm. Des.*, 2019, **25**, 3406–3416.
73 K. Senthilarasan, P. Sakthivel and A. Ragu, in *Recent Trends in Materials Science and Applications*, 2017, ch. 19, pp. 195–204, DOI: **10.1007/978-3-319-44890-9_19**.
74 A. Ahmad, N. M. Mubarak, F. T. Jannat, T. Ashfaq, C. Santulli, M. Rizwan, A. Najda, M. Bin-Jumah, M. M. Abdel-Daim, S. Hussain and S. Ali, *Processes*, 2021, **9**, 137.
75 J. Zhang, Q. Wang and A. Wang, *Acta Biomater.*, 2010, **6**, 445–454.
76 A. P. S. Prasanna and G. D. Venkatasubbu, *Prog. Biomater.*, 2018, **7**, 289–296.
77 G. Paradossi, F. Cavalieri, E. Chiessi, C. Spagnoli and M. K. Cowman, *J. Mater. Sci.: Mater. Med.*, 2003, **14**, 687–691.
78 P. Zou, S. Yuan, X. Yang, Y. Guo, L. Li, C. Xu, X. Zhai and J. Wang, *J. Funct. Foods*, 2019, **57**, 157–165.
79 V. Uskokovic and T. A. Desai, *J. Pharm. Sci.*, 2014, **103**, 567–579.
80 D. Feng, J. Shi, X. Wang, L. Zhang and S. Cao, *RSC Adv.*, 2013, **3**, 24975.
81 N. I. Farkas, L. Marincas, R. Barabas, L. Bizo, A. Ilea, G. L. Turdean, M. Tosa, O. Cadar and L. Barbu-Tudoran, *Materials*, 2022, **15**, 2105.
82 R. P. Das, V. V. Gandhi, B. G. Singh and A. Kunwar, *Curr. Pharm. Des.*, 2019, **25**, 3034–3056.
83 W. Sun, J. Fan, S. Wang, Y. Kang, J. Du and X. Peng, *ACS Appl. Mater. Interfaces*, 2018, **10**, 7832–7840.
84 Z. Luo, Y. Dai and H. Gao, *Acta Pharm. Sin. B*, 2019, **9**, 1099–1112.
85 L. Kong, Z. Mu, Y. Yu, L. Zhang and J. Hu, *RSC Adv.*, 2016, **6**, 101790–101799.
86 Y. Kang, W. Sun, J. Fan, Z. Wei, S. Wang, M. Li, Z. Zhang, Y. Xie, J. Du and X. Peng, *Mater. Chem. Front.*, 2018, **2**, 1791–1798.
87 Y. Liu, D. B. Raina, S. Sebastian, H. Nagesh, H. Isaksson, J. Engellau, L. Lidgren and M. Tägil, *Acta Biomater.*, 2021, **131**, 555–571.
88 A. Sirka, D. B. Raina, H. Isaksson, K. E. Tanner, A. Smailys, A. Kumar, S. Tarasevicius, M. Tagil and L. Lidgren, *Tissue Eng., Part A*, 2018, **24**, 1753–1764.
89 K. C. Hui, N. Dhanapalan, A. C. Khayrani, T. Imanto and N. S. Sambudi, *C. R. Chim.*, 2022, **25**, 295–306.
90 S. Jose, A. Joy, P. Devi, G. Unnikrishnan, M. Megha, M. Haris, K. Elayaraja and M. Senthilkumar, *Mater. Today: Proc.*, 2022, **58**, 836–845.
91 E. X. Figueroa-Rosales, J. Martínez-Juárez, E. García-Díaz, D. Hernández-Cruz, S. A. Sabinas-Hernández and M. J. Robles-Águila, *Crystals*, 2021, **11**, 832.
92 G. M. Neelgund and A. R. Oki, *J. Colloid Interface Sci.*, 2016, **484**, 135–145.
93 F. Mohandes and M. Salavati-Niasari, *J. Nanopart. Res.*, 2014, **16**, 2604.

94 D. A. C. Ferreira-Ermita, F. L. Valente, E. C. Carlo-Reis, F. R. Araújo, I. M. Ribeiro, C. C. V. Cintra and A. P. B. Borges, *Results Mater.*, 2020, **5**, 100063.
95 S. Mortazavi-Derazkola, M. Salavati-Niasari, H. Khojasteh, O. Amiri and S. M. Ghoreishi, *J. Cleaner Prod.*, 2017, **168**, 39–50.
96 A. E. Herrera-Alonso, M. C. Ibarra-Alonso, S. C. Esparza-Gonzalez, S. Estrada-Flores, L. A. Garcia-Cerda and A. Martinez-Luevanos, *Materials*, 2021, **14**, 6941.
97 L. Janovák, Á. Deák, S. P. Tallósy, D. Sebők, E. Csapó, K. Bohinc, A. Abram, I. Pálinkó and I. Dékány, *Surf. Coat. Technol.*, 2017, **326**, 316–326.
98 T. Matsumoto, M. Okazaki, A. Nakahira, J. Sasaki, H. Egusa and T. Sohmura, *Curr. Med. Chem.*, 2007, **14**, 2726–2733.
99 P. D. Costantino, C. D. Friedman, K. Jones, L. C. Chow, H. J. Pelzer and G. A. Sisson, *Arch. Otolaryngol., Head Neck Surg.*, 1991, **117**, 379–384.
100 G. Bharath, K. Rambabu, F. Banat, S. Anwer, S. Lee, N. BinSaleh, S. Latha and N. Ponpandian, *Mater. Res. Express*, 2019, **6**, 085409.
101 W. Suchanek and M. Yoshimura, *J. Mater. Res.*, 1998, **13**, 94–117.
102 T. Wang, D. Wang, J. Liu, B. Feng, F. Zhou, H. Zhang, L. Zhou, Q. Yin, Z. Zhang, Z. Cao, H. Yu and Y. Li, *Nano Lett.*, 2017, **17**, 5429–5436.
103 S. K. Lower, P. A. Maurice and S. J. Traina, *Geochim. Cosmochim. Acta*, 1998, **62**, 1773–1780.
104 D. C. Manatunga, R. M. de Silva, K. M. N. de Silva, N. de Silva, S. Bhandari, Y. K. Yap and N. P. Costha, *Eur. J. Pharm. Biopharm.*, 2017, **117**, 29–38.
105 W. Li, F. Han, H. Liu, X. Niu and L. Shi, *Ceram. Int.*, 2020, **46**, 28578–28584.
106 X. Hao, X. Hu, C. Zhang, S. Chen, Z. Li, X. Yang, H. Liu, G. Jia, D. Liu, K. Ge, X. J. Liang and J. Zhang, *ACS Nano*, 2015, **9**, 9614–9625.
107 M. Cao, Y. Wang, X. Hu, H. Gong, R. Li, H. Cox, J. Zhang, T. A. Waigh, H. Xu and J. R. Lu, *Biomacromolecules*, 2019, **20**, 3601–3610.
108 L. Zhou, Y. Zhang, D. Zeng, T. Shu and S. Wang, *J. Sol-Gel Sci. Technol.*, 2021, **97**, 600–609.
109 R. T. Shafranek, S. C. Millik, P. T. Smith, C.-U. Lee, A. J. Boydston and A. Nelson, *Prog. Polym. Sci.*, 2019, **93**, 36–67.
110 H. Ma, J. Shi, X. Zhu, Z. Zhang, J. Li and S. Cao, *Adv. Compos. Hybrid Mater.*, 2019, **2**, 242–253.
111 N. E. Aydin, *Int. J. Polym. Sci.*, 2020, **2020**, 1–13.
112 P. Kheirkhah, S. Denyer, A. D. Bhimani, G. D. Arnone, D. R. Esfahani, T. Aguilar, J. Zakrzewski, I. Venugopal, N. Habib, G. L. Gallia, A. Linninger, F. T. Charbel and A. I. Mehta, *Sci. Rep.*, 2018, **8**, 11417.
113 P. M. Price, W. E. Mahmoud, A. A. Al-Ghamdi and L. M. Bronstein, *Front. Chem.*, 2018, **6**, 619.
114 N. Saxena, N. Dholia, S. Akkireddy, A. Singh, U. C. S. Yadav and C. L. Dube, *Appl. Nanosci.*, 2019, **10**, 649–660.
115 B. Govindan, B. S. Latha, P. Nagamony, F. Ahmed, M. A. Saifi, A. H. Harrath, S. Alwasel, L. Mansour and E. H. Alsharaeh, *Nanomaterials*, 2017, **7**, 138.
116 H. Li, X. Sun, Y. Li, B. Li, C. Liang and H. Wang, *Mater. Sci. Eng., C*, 2019, **97**, 222–229.
117 S. Ramasamy, D. Dhamecha, K. Kaliyamoorthi, A. S. Pillai, A. Alexander, P. Dhanaraj, J. U. Menon and I. V. M. V. Enoch, *Mater. Adv.*, 2021, **2**, 3315–3327.
118 N. Petchsang, W. Pon-On, J. H. Hodak and I. M. Tang, *J. Magn. Magn. Mater.*, 2009, **321**, 1990–1995.
119 S. A. Hassanzadeh-Tabrizi, H. Norbakhsh, R. Pournajaf and M. Tayebi, *Ceram. Int.*, 2021, **47**, 18167–18176.
120 K. Naseri, E. Khademi and S. Mortazavi-Derazkola, *Arabian J. Chem.*, 2023, **16**, 104404.
121 A. Mushtaq, R. Zhao, D. Luo, E. Dempsey, X. Wang, M. Z. Iqbal and X. Kong, *Mater. Des.*, 2021, **197**, 109269.
122 Y. Liu, P. Bhattarai, Z. Dai and X. Chen, *Chem. Soc. Rev.*, 2019, **48**, 2053–2108.
123 S. Xu, J. Shi, D. Feng, L. Yang and S. Cao, *J. Mater. Chem. B*, 2014, **2**, 6500–6507.
124 Z. Song, Y. Liu, J. Shi, T. Ma, Z. Zhang, H. Ma and S. Cao, *Mater. Sci. Eng., C*, 2018, **83**, 90–98.
125 P. Song, W. Wang, J. Li, S. Cao and J. Shi, *Ceram. Int.*, 2022, **48**, 27957–27966.
126 R. Sang, M. Chen, Y. Yang, Y. Li, J. Shi, Y. Deng, X. Chen and W. Yang, *J. Biomed. Mater. Res., Part A*, 2019, **107**, 2296–2309.
127 X. Jiang, X. Liu, J. Cai, S. Wei, Y. Wang, Z. Duan, Z. Zhou, R. Sun, X. Qu and Y. Tang, *Colloids Surf., B*, 2023, **222**, 113097.
128 L. Benedini, D. Placente, J. Ruso and P. Messina, *Mater. Sci. Eng. C*, 2019, **99**, 180–190.
129 S. Shang, Q. Zhao, D. Zhang, R. Sun and Y. Tang, *Mater. Sci. Eng., C*, 2019, **105**, 110017.
130 S. Mohammadi-Aghdam, B. Valinezhad-Saghezi, Y. Mortazavi and S. M. Qhoreishi, *Drug Res.*, 2019, **69**, 93–99.
131 S. Ghosh, S. Ghosh and N. Pramanik, *Adv. Compos. Hybrid Mater.*, 2020, **3**, 303–314.
132 Q.-L. Tang, Y.-J. Zhu, J. Wu, F. Chen and S.-W. Cao, *Nanomedicine*, 2011, **7**, 428–434.
133 Y. H. Liang, C. H. Liu, S. H. Liao, Y. Y. Lin, H. W. Tang, S. Y. Liu, I. R. Lai and K. C. Wu, *ACS Appl. Mater. Interfaces*, 2012, **4**, 6720–6727.
134 J. Yoon, D. Kim, A. S. Siregar, B. Y. Lee, K.-Y. Kwon, J.-H. Byun and D. K. Woo, *Bull. Korean Chem. Soc.*, 2015, **36**, 445–446.
135 H. Hamada, H. Ohshima, A. Ito, W. I. Higuchi and M. Otsuka, *Biol. Pharm. Bull.*, 2010, **33**, 1228–1232.
136 T. Hebishima, S. Tada, S. N. Takeshima, T. Akaike, Y. Ito and Y. Aida, *Biochem. Biophys. Res. Commun.*, 2011, **415**, 597–601.
137 A. Behnamsani and A. Meshkini, *J. Drug Delivery Sci. Technol.*, 2019, **53**, 101200.
138 M. Xiaoyu, D. Xiuling, Z. Chunyu, S. Yi, Q. Jiangchao, Y. Yuan and L. Changsheng, *Nanoscale*, 2019, **11**, 15312–15325.
139 Y. M. Kang, G. H. Kim, J. I. Kim, D. Y. Kim, B. N. Lee, S. M. Yoon, J. H. Kim and M. S. Kim, *Biomaterials*, 2011, **32**, 4556–4564.

140 C. Zhang, W. Wang, T. Liu, Y. Wu, H. Guo, P. Wang, Q. Tian, Y. Wang and Z. Yuan, *Biomaterials*, 2012, **33**, 2187–2196.
141 B. Kundu, D. Ghosh, M. K. Sinha, P. S. Sen, V. K. Balla, N. Das and D. Basu, *Ceram. Int.*, 2013, **39**, 9557–9566.
142 Y. Yang, F. Xia, Y. Yang, B. Gong, A. Xie, Y. Shen and M. Zhu, *J. Mater. Chem. B*, 2017, **5**, 8600–8606.
143 M. Lelli, N. Roveri, C. Marzano, J. D. Hoeschele, A. Curci, N. Margiotta, V. Gandin and G. Natile, *Dalton Trans.*, 2016, **45**, 13187–13195.
144 Y. Tahara and Y. Ishii, *J. Orthop. Sci.*, 2001, **6**, 556–565.
145 D. A. Uchida, Y. Shinto, N. Araki and K. Ono, *J. Orthop. Res.*, 1992, **10**, 440–445.
146 Q. Zhang, L. Xiao and Y. Xiao, *Pharmaceutics*, 2021, **13**, 1572.
147 J. S. Son, M. Appleford, J. L. Ong, J. C. Wenke, J. M. Kim, S. H. Choi and D. S. Oh, *J. Controlled Release*, 2011, **153**, 133–140.
148 C. Zhou, Y. Hong and X. Zhang, *Biomater. Sci.*, 2013, **1**, 1012–1028.
149 J. B. Lee, S. H. Lee, S. M. Yu, J.-C. Park, J. B. Choi and J. K. Kim, *Surf. Coat. Technol.*, 2008, **202**, 5757–5761.
150 L. Xia, K. Lin, X. Jiang, Y. Xu, M. Zhang, J. Chang and Z. Zhang, *J. Mater. Chem. B*, 2013, **1**, 5403–5416.
151 T. Albrektsson and C. Johansson, *Eur. Spine J.*, 2001, **10**, S96–S101.
152 N. L. D'Elia, C. Mathieu, C. D. Hoemann, J. A. Laiuppa, G. E. Santillan and P. V. Messina, *Nanoscale*, 2015, **7**, 18751–18762.
153 R. Okabayashi, M. Nakamura, T. Okabayashi, Y. Tanaka, A. Nagai and K. Yamashita, *J. Biomed. Mater. Res., Part B*, 2009, **90**, 641–646.
154 I. Nadra, J. C. Mason, P. Philippidis, O. Florey, C. D. Smythe, G. M. McCarthy, R. C. Landis and D. O. Haskard, *Circ. Res.*, 2005, **96**, 1248–1256.
155 A. E. Ewence, M. Bootman, H. L. Roderick, J. N. Skepper, G. McCarthy, M. Epple, M. Neumann, C. M. Shanahan and D. Proudfoot, *Circ. Res.*, 2008, **103**, e28–e34.
156 C. M. Sayes, K. L. Reed and D. B. Warheit, *Toxicol. Sci.*, 2007, **97**, 163–180.
157 R. Service, *Science*, 2003, **300**, 243.
158 M. Motskin, D. M. Wright, K. Muller, N. Kyle, T. G. Gard, A. E. Porter and J. N. Skepper, *Biomaterials*, 2009, **30**, 3307–3317.